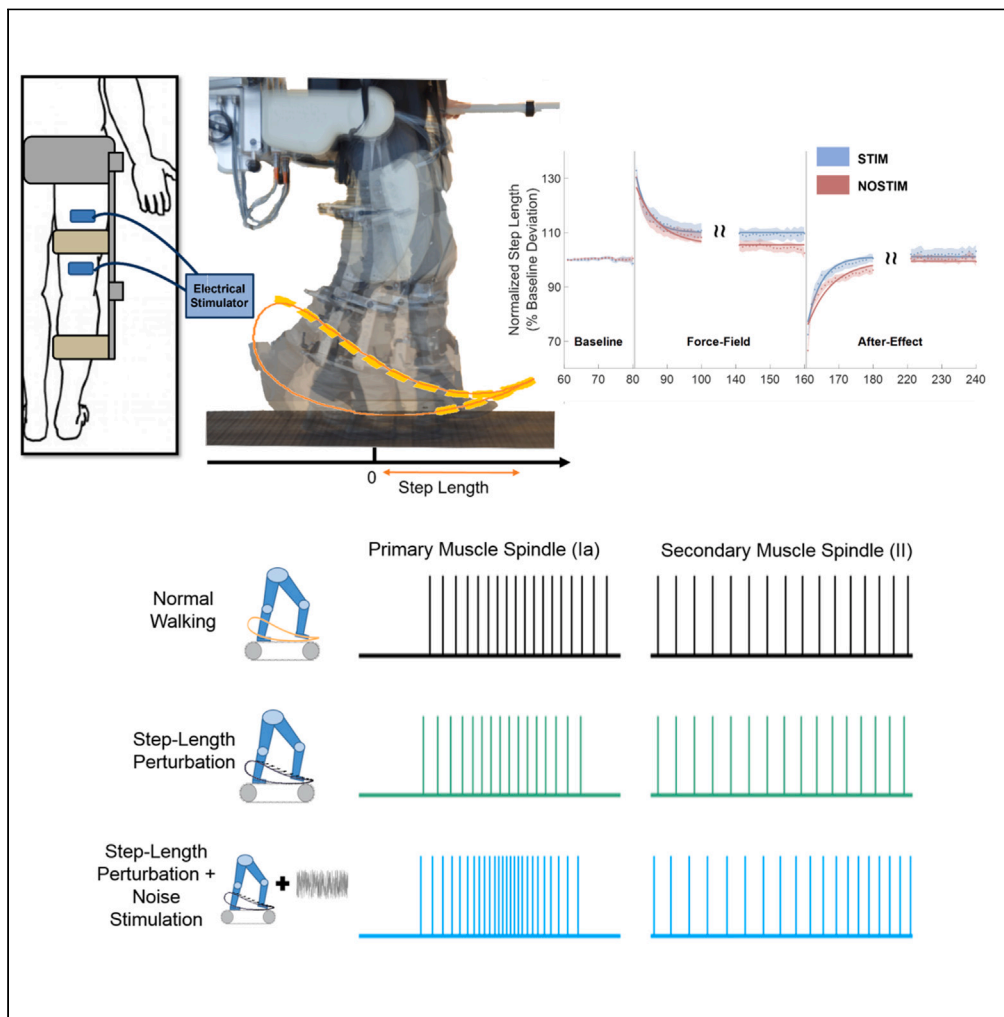# iScience

Article

Subsensory stochastic electrical stimulation targeting muscle afferents alters gait control during locomotor adaptations to haptic perturbations

Giacomo Severini,
Alexander Koenig,
Iahn Cajigas,
Nicholas
Lesniewski-Laas,
James Niemi,
Paolo Bonato

giacomo.severini@ucd.ie

Highlights

Subsensory electrical noise stimulation alters locomotor adaptation

Participants adapted faster but to a lesser extend when undergoing stimulation

The results suggest an effect of the stimulation on the muscle spindles

Subsensory stimulation can selectively alter the activity of the targeted muscles

Article

Subsensory stochastic electrical stimulation targeting muscle afferents alters gait control during locomotor adaptations to haptic perturbations

Giacomo Severini,[1,2,3,6,*] Alexander Koenig,[1] Iahn Cajigas,[1,4] Nicholas Lesniewski-Laas,[5] James Niemi,[5] and Paolo Bonato[1,5]

SUMMARY

Subsensory noise stimulation targeting sensory receptors has been shown to improve balance control in healthy and impaired individuals. However, the potential for application of this technique in other contexts is still unknown. Gait control and adaptation rely heavily on the input from proprioceptive organs in the muscles and joints. Here we investigated the use of subsensory noise stimulation as a means to influence motor control by altering proprioception during locomotor adaptations to forces delivered by a robot. The forces increase step length unilaterally and trigger an adaptive response that restores the original symmetry. Healthy participants performed two adaptation experiments, one with stimulation applied to the hamstring muscles and one without. We found that participants adapted faster but to a lesser extent when undergoing stimulation. We argue that this behavior is because of the dual effect that the stimulation has on the afferents encoding position and velocity in the muscle spindles.

INTRODUCTION

Subsensory mechanical and electrical noise stimulation targeting sensory receptors can alter the kinesthetic sense and lead to improved motor performance.[1–4] This effect is understood to be related to the stochastic resonance phenomenon, for which small amounts of noise can improve the detection of weak signals in nonlinear threshold-based systems.[5,6] The noise, if correctly calibrated, increases the sensitivity of the threshold-based system, allowing for the detection of otherwise undetectable signals. An optimal level of noise maximizes this effect. Stochastic resonance has been observed to occur in response to noise stimulation in threshold-based biological systems,[5] in neurons[7] and in human sensory receptors.[8] It is believed that noise applied mechanically or electrically to sensory receptors boosts proprioception by depolarizing the associated afferents and facilitating their firing and the transmission of the sensory information to the central nervous system (CNS).

Mechanical and electrical stimulation targeting joints, muscles and the soles of the feet, has been consistently shown to improve posturographic parameters during different balance exercises.[1,2,9–17] However, the application of this technique to lower extremity tasks different than balance has been more limited,[4,18–21] making it unclear whether subsensory stimulation can be successfully used also in other contexts and whether it can be selectively used to elicit desired changes in the motor behaviors associated with the performance of dynamic tasks.

Proprioceptive feedback plays a crucial role during locomotion, regulating the magnitude and duration of the activity of the various flexor and extensor muscles.[22–25] Proprioception is also central during lower limb motor adaptations, by generating the kinesthetic component of the sensory prediction error that drives adaptation.[26] It has been also observed that locomotor adaptation during split-belt treadmill experiments is associated with a recalibration of the perception of limb speed,[27,28] a process that has been attributed to the cerebellum.[29] Given its dependence on proprioceptive input, locomotor adaptation appears to be an appropriate task to test whether the use of subsensory noise stimulation to boost proprioception affects dynamic motor control.

Based on this rationale, we tested the use of subsensory electric current applied directly on the surface of the hamstring muscles for the purpose of altering the response of healthy individuals to a unilateral haptic

[1]Department of Physical Medicine & Rehabilitation, Harvard Medical School, Spaulding Rehabilitation Hospital, Boston, MA, USA

[2]School of Electrical and Electronic Engineering, University College Dublin, Dublin, Dublin 4, Ireland

[3]Centre for Biomedical Engineering, University College Dublin, Dublin, Dublin 4, Ireland

[4]Department of Neurological Surgery, University of Pennsylvania, Philadelphia, PA, USA

[5]Wyss Institute for Biologically Inspired Engineering, Harvard University, Boston, MA, USA

[6]Lead contact

*Correspondence: giacomo.severini@ucd.ie

https://doi.org/10.1016/j.isci.2023.107038

perturbation delivered using a commercial robot for gait rehabilitation. The participants underwent two experiments consisting in walking while experiencing the perturbation, one with and one without the sub-sensory stimulation. The perturbation was active during the swing phase of the gait cycle and had the effect of increasing the step length of the participants' right foot and triggering an adaptive process aiming at restoring the original step length, following a known paradigm.[30,31] We analyzed adaptation in step length together with the associated kinematics and kinetics to clarify whether changes because of the stimulation correlate with a modification in the activity of the hamstring muscles.

We hypothesized that the subsensory electrical stimulation would hyperpolarize the muscle spindles, increasing their sensitivity, thus modifying adaptation performance. This modified adaptation performance would be expressed as a faster adaptation process because of the increase in the amount of proprioceptive information available from a group of muscles involved in the adaptation process.[31] As expected from our hypothesis, we found that the stimulation leads to faster adaptations. However, to our own surprise, we observed that the faster adaptation converged toward a longer residual step length, indicating a less complete adaptation process. The faster adaptation could be because of the increase in available propriocep-tive information, as per our hypothesis, and/or from the larger target residual step length. Given this obser-vation, these results cannot fully confirm our initial hypothesis. We theorize that our results may depend on the differential effect that the stimulation has on the different sensory receptors present in the muscle spin-dles, although future studies are necessary to confirm this. These results may have implications on the use of subsensory stimulation during robot-assisted gait therapy of individuals presenting with proprioceptive deficits.

RESULTS

Experimental setup, testing protocol, and analyses

In this study, 30 healthy individuals (15 women, average age = 27.4 $\pm$ 3.8, average BMI = 22.9 $\pm$ 2) per-formed two locomotor adaptation experiments using the Lokomat device (Hocoma, Switzerland), a commercially available robot designed for administering robot-assisted gait training.[32] Participants per-formed one locomotor adaptation experiment while experiencing subsensory electrical stimulation during the whole experiment (STIM condition) and one while experiencing the stimulation only in the first 20 s of the experiment (NOSTIM condition). The two experiments were carried out in different days and in a random order, with the participants unaware of the condition associated with each experiment. Thus, the electrodes and stimulator were set up and started during both experiments, but for the NOSTIM exper-iment the stimulation was shut down after 20 s.

During each locomotor adaptation experiment, participants experienced 80 steps of unperturbed walking (Baseline phase) during which the robot was fully back-driven and compensating for the interaction forces between itself and the user. These steps were followed by 80 steps of perturbed walking (Force-field phase), and finally 80 steps of unperturbed walking (After-effect phase) during which the robot was once again fully back-driven. The perturbation, whose effects have been examined in previous studies,[30,31] was designed as a velocity-dependent force-field acting on the right leg during the swing phase. The net effect of the perturbation was to increase the step length of the right foot (Figure 1A). The magnitude of the force-field was dependent on the weight of the participant and was tuned so as to induce a step length increase of approximately 30% with respect to the baseline step length.[30] During both locomotor adaptation experiments, a pair of electrodes for electrical stimulation were placed on the participants' hamstrings (Figure 1B). In both experimental conditions, participants received subsensory electrical stim-ulation consisting of zero mean Gaussian white noise with RMS amplitude value set at 90% of the sensory threshold (estimated as 191.3 $\pm$ 144.8 µA through all the experiments of all the participants). The frequency of the applied stimulation had a bandwidth of (0 Hz, 1kHz] and was the same for all subjects. Each exper-iment lasted for about 10 min. As in previous studies based on the same paradigm,[30,31] the adaptation to the perturbation was quantified as the change in step length observed during the different phases of the experiments. Step length was calculated from the joint angles measured by the robot (see STAR Methods) in a Cartesian coordinate system with origin at the hip joint of the robot. The estimated length of each step taken by study participants was normalized and expressed as percentage change with respect to the average step length observed during the baseline phase of each experiment. Adaptation and de-adapta-tion are usually characterized by a marked exponential-like trend.[30] For this reason, adaptation and de-adaptation behaviors were modeled by fitting exponential functions (Figures 1C and Equation 4) to the data recorded during the Force-field and After-effect phases of the experiments. The timing of adaptation
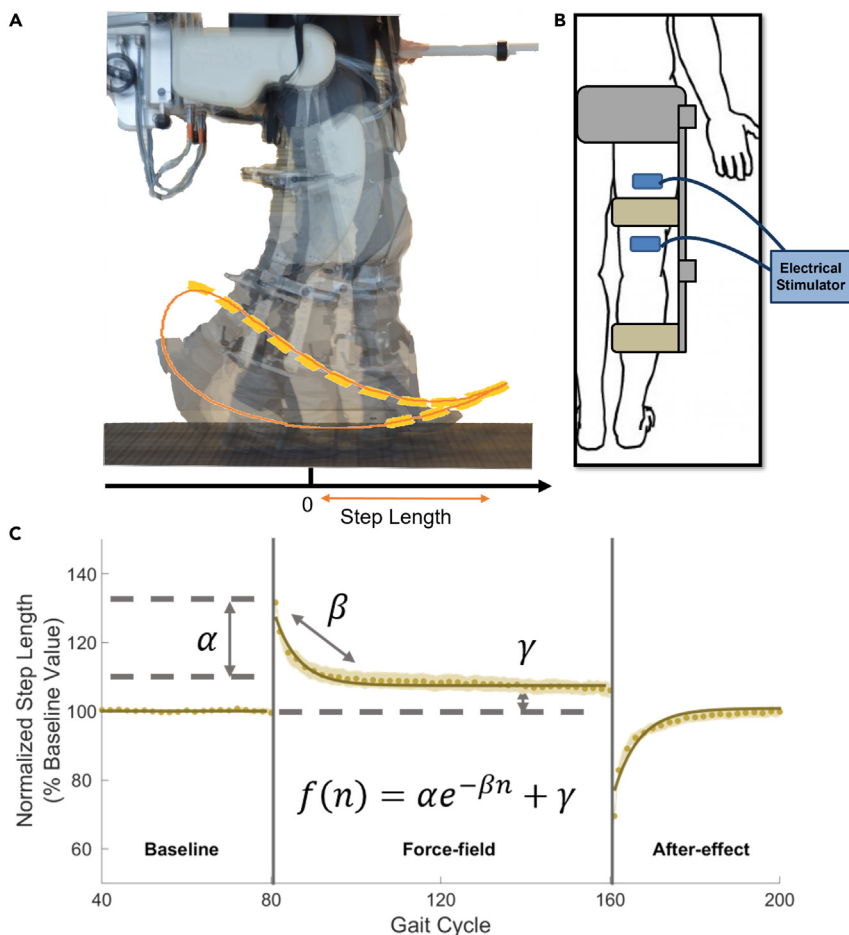
Figure 1. Experimental Setup and Metrics

(A) Lokomat setup for the motor adaptation experiment. Calculation of step length was performed in the reference system of the Lokomat, with the zero set at the mechanical center of the hip joint. The perturbing force-field (indicated by the yellow beams over the orange foot trajectory) was active during the swing phase of the gait cycle.

(B) The electrodes for SR stimulation were placed approximately 5 cm above and below the tight upper cuff on the back of the right leg of each participant, targeting the hamstrings.

(C) Amount and rate of adaptation and de-adaptation were calculated from the normalized step length and were modeled using the exponential function in the equation.

and de-adaptation was estimated from the time constant of the fitted exponentials, as a mean to verify our hypothesis. We also analyzed the values of normalized step length in specific sections of the experiments. In our analyses, we first compared the changes in step length and gait biomechanics between the STIM and NOSTIM conditions, regardless of which condition was experienced first. We also analyzed differences between the two stimulation conditions by stratifying the participants in two groups, based on the order of the two experiments (STIM first or NOSTIM first).

Analysis of the effect of the stimulation conditions on step length adaptation

When comparing the two stimulation conditions regardless of order, we found two distinct behaviors in the adaptation plots for the STIM and NOSTIM conditions (Figure 2A). Specifically, in the Force-field phase, we observed exponential changes in step length that converged faster and toward a higher target step length in the STIM condition compared to the NOSTIM condition. This observation suggests that participants, during the STIM condition, adapted faster but to a less extent compared to the NOSTIM condition. Figure 2B shows the time constants of adaptation associated with the exponential fittings performed on the average step length data for the complete STIM and NOSTIM datasets. The number of steps needed for adaptation were estimated as 3 times the time constant β of the exponential function fitted to the data.
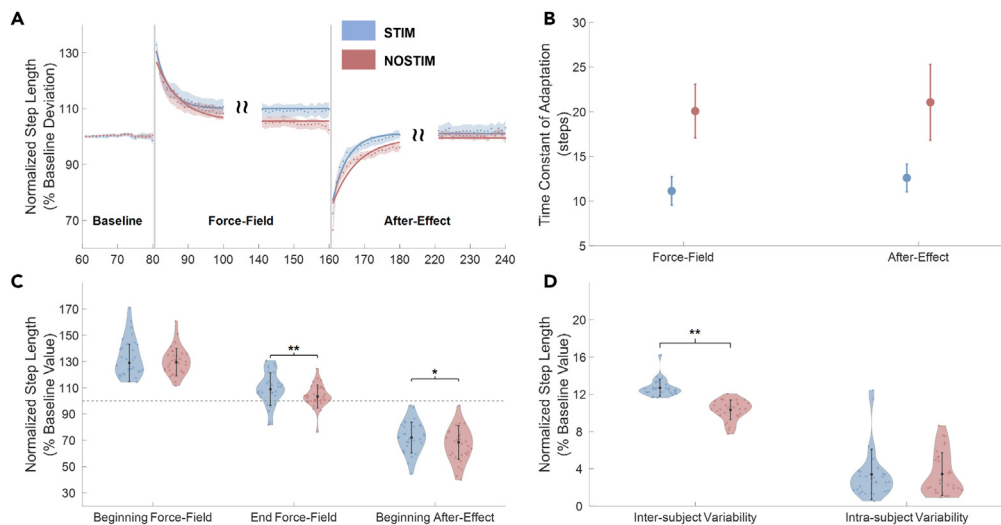
Figure 2. Analysis of step length adaptation, STIM versus NOSTIM conditions

(A) Step length changes over the course of the experiment for the STIM (light blue) and NOTISM (light red) conditions. Dots and shaded areas represent average and standard error of the normalized step length across all participants for each condition. Bold lines represent the exponential fitting calculated from the average data of each condition. Two different behaviors are clearly identifiable between the STIM and NOTISM conditions.

(B) Time constants (in steps ±95% confidence interval) of the exponentials estimated during the Force-field and After-Effect phases for the STIM and NOSTIM conditions. The STIM condition presents faster adaptation and de-adaptation time constants.

(C) Across-participants average ±standard deviation of step length at the beginning and end of the Force-Field and at the beginning of the After-Effect. The STIM condition presented significant higher residual step length at the end of the Force-Field and significantly lower initial After-Effect with respect to the NOSTIM condition, indicating a smaller extent of adaptation. Error bars represent median ±standard deviation across participants.

(D) Inter-subject and intra-subject variability in step length. STIM condition is associated with a significant higher inter-subject variability, whereas intra-subject variability is un-altered between the two conditions. Error bars represent median ± standard deviation across participants.

From the analysis of the time constant derived from the fitted exponentials, expressed as the estimated value of steps ±95% confidence interval, we found that participants took approximately 11.1 ± 1.6 steps (rmse = 0.06) to adapt to the perturbation in the STIM condition, whereas 20.1 ± 3.0 steps were needed in the NOSTIM condition (rmse = 0.10). Similarly, in the After-effect phase, participants took approximately 12.6 ± 1.5 steps rmse = 0.10) to de-adapt the modified gait pattern in the STIM condition, whereas 21.1 ± 4.2 steps were needed in the NOSTIM experiment to achieve the same result (rmse = 0.02).

Figure 2C shows the results of the statistical analysis performed to compare the step length values observed at different points of the experiments in the STIM and NOSTIM conditions. At the first step of the Force-field phase, participants showed a normalized step length value of 132.9 ± 14.2% for the STIM condition and of 130.4 ± 10.4% for the NOSTIM condition. This difference was not significant (p = 0.185, Wilcoxon's signed rank test with Bonferroni-Holm correction). The average step length across the last five steps of adaptation was 109.4 ± 12.1% for the STIM condition and 103.9 ± 9.1% for the NOSTIM condition. This difference was shown to be statistically significant (p = 0.024, Wilcoxon signed rank test with Bonferroni-Holm correction), supporting the preliminary observation that participants adapted to a lesser extent during the STIM condition. At the beginning of the After-effect phase, we observed a step length of 72.5 ± 11.7% for the STIM condition and 67.6 ± 12.8% for the NOSTIM condition. This difference was statistically significant (p = 0.04, Wilcoxon's signed rank test with Bonferroni-Holm correction) and may be explained by the smaller amount of adaptation observed for the STIM condition at the end of the Force-field phase. Figure 2D presents the analysis of the inter-subject and intra-subject variability in step length at the end of the Force-field phase. We calculated inter-subject variability in step length as the standard deviation across participants of the average step length observed in the last 30 steps of the Force-field phase. For the STIM condition, we observed a value of inter-subject variability equal to 12.7 ± 0.9% compared to 10.3 ± 1.0% for the NOSTIM condition. This difference was shown to be

statistically significant with a p < 0.001 (Wilcoxon's signed rank test with Bonferroni-Holm correction). Intra-subject variability was calculated as the standard deviation of step length across steps observed in the last 30 steps of the Force-field phase. For this parameter, we did not observe significant differences between the STIM and NOSTIM conditions, with values of 3.4 ± 2.7% for the former and 3.4 ± 2.3% for the latter (p = 0.688, Wilcoxon's signed rank test with Bonferroni-Holm correction). These results suggest an increase in variability between the different participants when exposed to stimulation. This increase however does not appear to be caused by an increase in the intrinsic step-by-step variability of each participant.

The main result of the analysis presented in this paragraph is that the STIM condition is associated with a faster but less complete adaptation with respect to NOSTIM. To control whether the faster adaptation time constant is because of the higher residual step length at the end of the adaptation period, we re-calculated the time constant of adaptation for NOSTIM up to the point in the data where the residual step length observed in STIM is reached. In this analysis we first added to the NOSTIM data the difference in step length observed at the first step of adaptation between the STIM and NOSTIM conditions. This was done to account for the higher initial step-length observed during STIM. We then fitted the exponential function on the portion of the NOSTIM data up to the third occurrence of step length values below the value of residual step length calculated at the end of the STIM condition. This analysis, presented in Figure S3 in the supplemental information, show that STIM is still associated with a slightly faster adaptation time constant (11.1 ± 1.25 steps rmse = 0.06) with respect to NOSTIM (12 ± 1.55 steps, rmse = 0.08).

Session-dependent analysis

Locomotor adaptations can present savings, which is a phenomenon where an adaptation experiment experienced after an earlier one is characterized by a smaller initial error and a faster adaptation speed.[33] To account for the presence of savings, we analyzed the dataset by stratifying participants depending on the order of the experiments. In this analysis, we split the datasets depending on whether the participants experienced the STIM or NOSTIM experiment in the first experiment and assessed each group (STIM-First and NOSTIM-First) of 15 participants separately. The results are presented in Figure 3, where blue and red indicate the STIM and NOSTIM conditions and light and dark color represent, respectively, the order of the experiment (first or second). The adaptation plots (Figure 3A) for the session-dependent analysis present adaptation trends consistent with those observed in the complete analysis. Specifically, the two STIM step length plots are "above" the respective NOSTIM datasets in the Force-field phase indicating a faster but less extent of adaptation. The analysis of the time constants confirmed this observation. The STIM-First group, in fact, presented a time constant of adaptation equal to 8.8 ± 1.9 steps for the STIM condition and 25.0 ± 3.0 steps for the NOSTIM condition (rmse = 0.08 and 0.15 respectively). The NOSTIM-First group presented the same directional trend of STIM adaptation being faster than the NOSTIM one, with a time constant of 15.8 ± 1.8 steps for the STIM condition and of 16.9 ± 0.8 steps for the NOSTIM condition. However, in this case, the confidence intervals of the estimation overlap considerably (rmse = 0.03 for STIM and rmse = 0.05 for NOSTIM). We also observed the same behavior in the time constants of the After-effect with faster time constant associated with the STIM conditions for both groups (16.6 ± 2.6 steps for the STIM-First group, 8.8 ± 1.0 steps for the NOSTIM-First group) compared to the NOSTIM conditions (26.7 ± 4.8 steps for the STIM-First group, 19.6 ± 1.7 steps for the NOSTIM-First group). The analysis of step length showed no substantial differences across the different groups in the initial response to the perturbation. The STIM-First group presented an initial deviation of 136.1 ± 4.2% in the STIM condition and of 132.1 ± 2.7% in the NOSTIM condition (p = 0.303, Wilcoxon's signed rank test with Bonferroni-Holm correction). Similarly, the NOSTIM-First group presented an initial deviation of 129.6 ± 2.6% in the STIM condition and of 128.7 ± 2.5% in the NOSTIM condition (p = 0.978, Wilcoxon's signed rank test with Bonferroni-Holm correction). At the end of the Force-field phase, participants in the STIM-First group presented a residual step length of 110.0 ± 3.6% in the STIM condition and of 102.7 ± 2.5% in the NOSTIM condition. This difference, however, was not statistically significant (p = 0.0520, Wilcoxon's signed rank test with Bonferroni-Holm correction). In the NOSTIM-First group, we observed a residual step length of 108.9 ± 2.9% in the STIM condition and of 105.8 ± 2.2% in the NOSTIM condition, although in this case the difference was not significant (p = 0.909, Wilcoxon's signed rank test with Bonferroni-Holm correction). At the beginning of the After-effect phase, we observed, for the STIM-First group, a step length equal to 70.6 ± 3.4% in the STIM condition and equal to 62.2 ± 2.9% in the NOSTIM condition. In the NOSTIM-first condition, we observed values for step length equal to 74.4 ± 2.4% and 71.0 ± 3.2% for the STIM and NOSTIM conditions. Only the differences observed for the STIM-first group were shown to be statistically significant (p = 0.039 for the STIM-First group, p = 0.978 for the NOSTIM-First group,
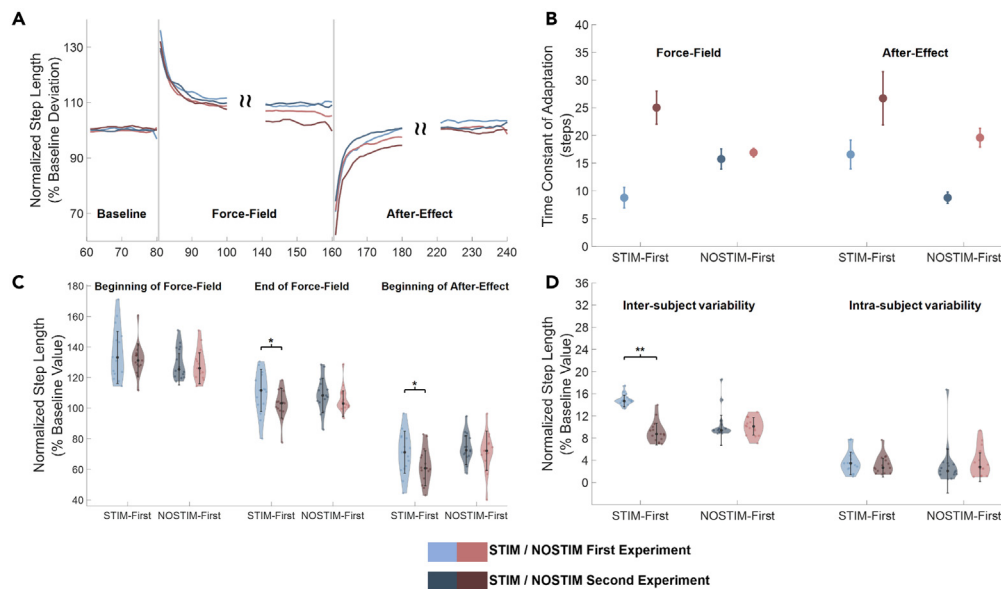
Figure 3. Session-dependent analysis of step length adaptation, STIM-First and NOSTIM-First groups

(A) Adaptation plots for the STIM (blue) and NOSTIM (red) conditions depending on the order of the experiment. Lighter color indicates that a condition has been experienced in the first experiment, while darker color in the second. Both STIM conditions present faster and less extended adaptation with respect to the respective NOSTIM conditions.

(B) Time constants (in steps ± 95% confidence interval) of the exponentials estimated during the Force-field and After-Effect phases for the STIM and NOSTIM conditions of the STIM-First and NOSTIM -First groups. The STIM conditions present faster adaptation and de-adaptation time constants in both groups.

(C) Across-participants average ± standard deviation of step length at the beginning and end of the Force-Field and at the beginning of the After-Effect. The STIM conditions presented higher residual step length at the end of the Force-Field and significantly lower initial After-Effect with respect to the respective NOSTIM conditions. This result was statistically significant (p < 0.05, Wilcoxon signed rank test) only for the STIM-First group. Error bars represent median ± standard deviation across participants.

(D) Inter-subject and intra-subject variability in step length. STIM condition for the STIM-First group presented a statistically significant higher inter-subject variability. Error bars represent median ± standard deviation across participants.

Wilcoxon's signed rank test with Bonferroni-Holm correction). Analysis of inter-subject variability (Figure 3D) showed statistically significant differences between the two stimulation conditions in the STIM-First group (15.2 ± 0.9% for STIM, 8.1 ± 1.6% for NOSTIM, p < 0.001, Wilcoxon's signed rank test) but not in the NOSTIM-First group (9.9 ± 2.0% for STIM, 11.9 ± 2.2% for NOSTIM, p = 0.454, Wilcoxon's signed rank test). Intra-subject variability did not present statistically significant differences between conditions for both groups, with values of 3.0 ± 2.0% for STIM and 2.67 ± 1.6% for NOSTIM in the STIM-First group (p = 0.978, Wilcoxon's signed rank test) and 3.0 ± 4.1% for STIM and 3.0 ± 2.0 for NOSTIM in the NOSTIM-First group (p = 0.909, Wilcoxon's signed rank test).

Effect of the stochastic resonance stimulation on the joint kinematics and kinetics at the hip and knee during adaptation

We analyzed the joint biomechanics to identify a possible cause of the differences in step length adaptation between the STIM and NOSTIM conditions. The average joint angles at the end of the adaptation period are similar in both conditions. The higher residual step length observed in the STIM condition compared to the NOSTIM condition is mainly explained by a slight increase in hip flexion and knee extension during STIM observed from about 40% of the gait cycle on. In particular, we observed an anticipation of the position of the peak hip flexion during swing in STIM with respect to NOSTIM (Table S1), which however was not significant after adjusting for multiple comparisons. We did not observe substantial differences in the measured torques at both the hip and knee between baseline and the last steps of adaptation in both conditions. It needs to be pointed out that the measured torques are the interaction torques between the user and the robot measured by the Lokomat sensors and do not capture completely the torques generated at the hip and knee during gait. We observed small, non-significant, differences between the

STIM and NOSTIM conditions for the hip torque. These differences were mostly characterized by a higher negative peak during late stance in STIM and an anticipated torque profile, which agrees with what observed in the kinematics.

At the knee, for both the STIM and NOSTIM conditions, we observed an increased peak knee torque during swing, which was higher for STIM compared to NOSTIM. In STIM, we also observed a lower negative peak during terminal swing, which appeared delayed in NOSTIM. Both these results were not statistically significant (Table S1). Adaptation to the perturbation is associated with an increase in joint power generated against the machine during the swing phase at both the hip and knees. At the knee level, in particular, a peak of generated power is present in late swing where normally a power absorption is observed. This behavior reflects the participants rejection of the step lengthening perturbation. Small differences, not statistically significant, were observed between the two conditions, with STIM associated with an anticipated hip power generation profile and a higher knee power peak during late swing. We estimated the power required to counteract the perturbation as the difference between the average power calculated during the baseline phase and that calculated in the last 5 steps of the adaptation phase, minus the power attributed to the perturbation itself (see STAR Methods for details). We observed, for both hip and knee and in both STIM and NOSTIM conditions, that participants exerted additional power at the beginning of the stance phase (loading-response) and during mid/terminal swing, when the perturbation is active. For both conditions the amount of additional power was higher at the knee with respect to the hip. At the hip we observed a higher amount of power exerted by the participants during the NOSTIM condition with respect to the STIM one. This difference was shown to be not significant (see supplemental information, Figure S1). At the knee, on the other hand, participants presented a higher additional power during the STIM condition with respect to the NOSTIM condition (Figure S1), but also this difference was not found to be statistically significant.

DISCUSSION

This study investigated the effect of subsensory electrical noise stimulation applied to the hamstring muscles during a robot-based locomotor adaptation experiment. Our results revealed that subsensory stimulation directly altered the adaptation process so that in the experiments where the stimulation was applied, individuals adapted faster but to a lesser extent compared to experiments during which no stimulation was delivered. We also saw that this effect is bigger in the group that received the stimulation in their first experiment. Our hypothesis was that the subsensory electrical stimulation would increase the sensitivity of the muscle spindles and thus accelerate the adaptation process by increasing the amount of proprioceptive information available to the CNS when processing and responding to the perturbation.

Although our results seem to confirm this hypothesis the reasons behind the accelerated adaptation that we observed are not completely clear. In fact, the observed increase in adaptation speed could be directly because of the stimulation or could be secondary to the larger kinematic error observed at the end of the force-field period in the STIM condition. The analysis of the time constant of adaptation after controlling for the difference in residual step-length (Figure S3) suggests that adaptation during the STIM condition is slightly faster than that observed the NOSTIM condition. However, the differences observed are minimal and this post-hoc analysis cannot completely exclude an effect of residual step length on adaptation speed. This effect can only be confirmed or excluded by an ad-hoc experiment controlling for the target adaptation step length. Nevertheless, if the adaptation during the STIM condition is indeed faster, the direct effect of the peripheral stimulation would be that of accelerating the adaptation process. The alternative possibility is that the smaller number of steps required to reach the adapted plateau would be a by-product of the fact that the adaptation target is closer to the original deviation induced by the perturbation.

In the following, we will discuss these two possible mechanisms. During motor adaptations to perturbations that induce dynamic changes in the walking environment, the CNS modifies the motor plan so as to anticipate the expected effects of the perturbation with the aim of minimizing the sensory prediction error associated with the kinematic error. In our experiments we induced a kinematic error in step length that leads to an asymmetric gait pattern. Adaptation in this case is likely associated with the restoration of the normal relationship between the center of mass and the boundaries of the base of support to maintain a stable gait pattern.[30,34] Emken et al. showed that motor adaptations during walking can be described as a tradeoff between the kinematic error caused by the perturbation and the effort required to reject it.[35] The same authors demonstrated that the rate of adaptation, herein measured by the number of steps needed

for the adaptation process to converge, depends on the magnitude of the perturbing force-field,[36] where stronger perturbations cause bigger kinematic errors and thus faster adaptation processes.

Rate of adaptation has also been shown to depend on the presence and structure of previous exposures to the perturbation.[33] Specifically, Malone et al. showed that individuals who had experienced multiple exposures to the same perturbation in the same day presented faster adaptations in the exposures following the first one, in a process often referred to as "savings".[33] We designed our experiments so as to limit the possible effects of savings by performing the adaptation experiments over non-consecutive days. Savings, however, have been observed also in case of experiments performed months apart.[37]

At a first glance, our data surprisingly showed a pattern opposite to the one observed by Malone. Our data shows that locomotor adaptation experiments performed in the second session (across both stimulation conditions) presented longer adaptation time constants with respect to those performed in the first session (Figure S2). However, this behavior appears to be driven by the group who received the stimulation in their first experimental session. Although we observed consistently faster but less "complete" adaptation in the STIM compared to the NOSTIM condition regardless of the order of the experiment, the STIM-first group presented the fastest learning time constant among session/conditions during STIM and the slowest during NOSTIM. This result may suggest that the stimulation is more effective if the task has not been experienced recently and that having first adapted with a "boosted" proprioceptive input disrupts a subsequent adaptation, possibly by disrupting the sensory recalibration process associated with locomotor adaptation.[27] This interpretation, although plausible, needs to be confirmed through specifically designed experiments.

The main proxies of the differences we observed between the step length adaptation processes in the STIM and NOSTIM conditions are the differences we observed in the kinematics and kinetics of the participants at the hip and knee joints. In the STIM condition, participants showed trends of slightly anticipated hip and knee angle patterns and increased knee torque and power generated during the late swing phase compared to the NOSTIM condition (Figure 4). These results show a difference in power exerted at the knee between the STIM and NOSTIM conditions (Figures 4 and S1). The behavior observed in the STIM condition is in accordance with an anticipation in negative knee torque production in swing (when the perturbation is active) and thus consistent with a higher (and possibly anticipated) activity of the hamstring muscles that are the main drivers of the negative contribution to the active knee torque in terminal swing, and that are the muscles we observed to contribute to the rejection of this particular perturbation.[31] Although the results of our experiments cannot directly confirm that the stimulation ultimately leads to an increased activity of the hamstrings, because EMG data was not recorded this plausible result, if verified, would clearly indicate that subsensory stimulation can be used to selectively alter the activity of different muscles during the performance of dynamic tasks.

To get a better understanding of the processes potentially leading to our results, it is perhaps useful to consider the theoretical effects that the subsensory electrical stimulation has on the muscle spindles during movement (Figure 5). Muscle spindles are intrafusal fibers parallel to the skeletal muscle fibers that encode information regarding the rate of muscle stretch (group Ia afferents) and the amount of muscle stretch (group II afferents) during active and passive contractions.[38] Specifically, the firing rate of group Ia afferents increases with the rate of muscle stretch, whereas that of group II afferents increases with the amount of stretch. Considering the hamstring muscles during the mid-to-terminal swing phase of the gait cycle, where the muscle is lengthening because of knee extension while contracting eccentrically, we can hypothesize the dynamic behavior of the stretch to be roughly proportional to the dynamical behavior of the knee angle. This gross approximation, that omits for simplicity these muscles' length dependency on the hip angle, which, however, does not change substantially in late swing, is herein used to emphasize the role that the hamstring muscles have in terminal swing, where they contribute to the deceleration of knee extension.

A perturbation like the one we applied in our experiment directly modifies the dynamic stretching of the hamstring muscles. As the perturbation increases step length mostly by exerting a knee-extending torque during swing, it induces a faster and higher stretch in the hamstring muscles before its compensation, thus driving higher firing rates in both the Ia and II receptors (Figure 5), with respect to their firing patterns during baseline walking. Small electrical currents acting on the spindles theoretically lead to a partial depolarization of the receptor membrane,[2,8] bringing it closer to its firing threshold. This effect should facilitate the firing of the receptors and possibly translate in both the Ia and II receptors firing at a higher firing rate given
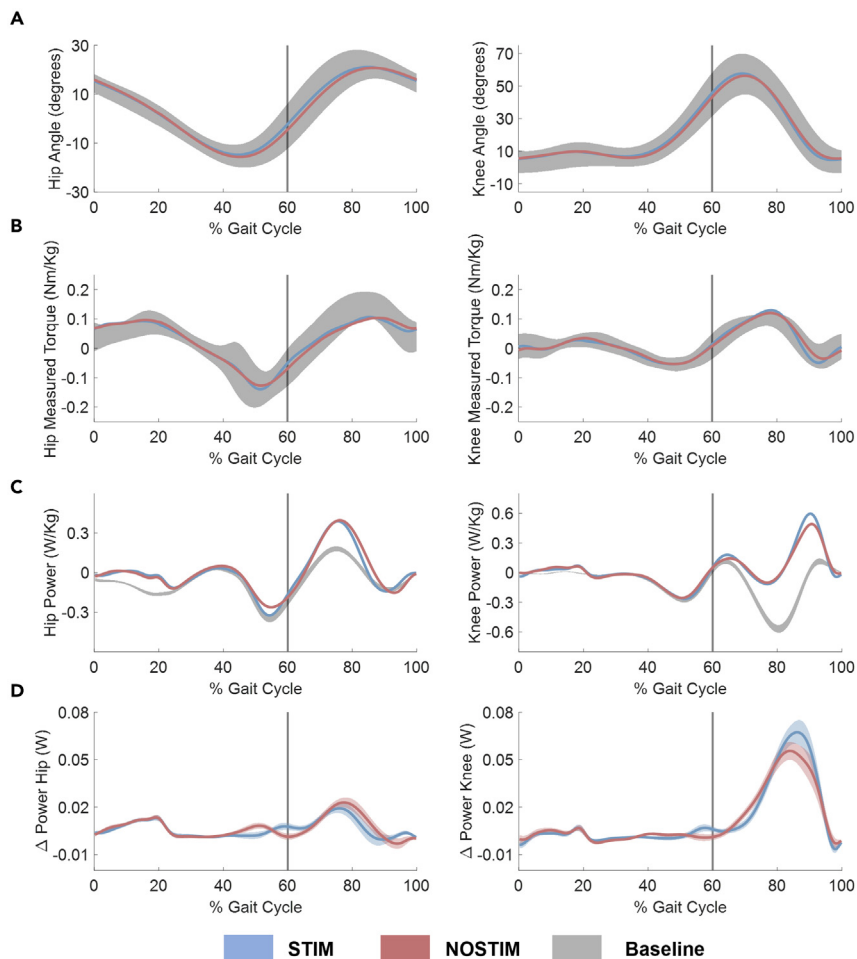
Figure 4. Hip/knee kinematics and kinetics during baseline and late adaptation

(A) Across-participants average hip (left) and knee (right) angles during baseline (shaded area represents the average ±
standard deviation across all participants) and at the end of adaptation for the STIM (blue line) and NOSTIM (red line)
groups (each line represents the average across participants).

(B) Across-participants average hip (left) and knee (right) measured torques during baseline (shaded area represents the
average ± standard deviation across all participants) and at the end of adaptation for the STIM (blue line) and NOSTIM
(red line) groups (each line represents the average across participants). The torques are measured as the interaction
torques between the individuals and the Lokomat exoskeleton and do not correspond to the joint torques.

(C) Across-participants average hip (left) and knee (right) power during baseline (shaded area represents the average ±
standard deviation across all participants) and at the end of adaptation for the STIM (blue line) and NOSTIM (red line)
groups (each line represents the average across participants). The power is calculated from the measured torques and do
not correspond to the actual joint power.

(D) Average ± standard deviation of the additional power (calculated as the difference between the power at the end of
adaptation and the power at baseline after removing the power associated with the erturbation) for the STIM (blue) and
NOSTIM (red) conditions at the hip (left) and knee (right). The STIM condition is characterized by a slightly lower peak hip
additional power, and by a significantly (see Figure S1) higher additional power at the knee level. In all eight plots the
vertical gray line represents the estimated point of transition between stance and swing phases of the gait cycle (toe-off).

the same rate and amount of stretch compared to their normal firing patterns. Thus, in this theorization,
the depolarization disrupts the natural coding between the firing rate of the Ia and II receptors and the
rate/amount of muscle stretch in the hamstrings, increasing the firing rate during the portion of the gait
pattern where the muscle is lengthening.

This theoretical framework suggests a coupled effect of the stimulation on the rate of adaptation. The
increased sensitivity of Ia receptors could, in fact, alter the perceived magnitude of the perturbation,
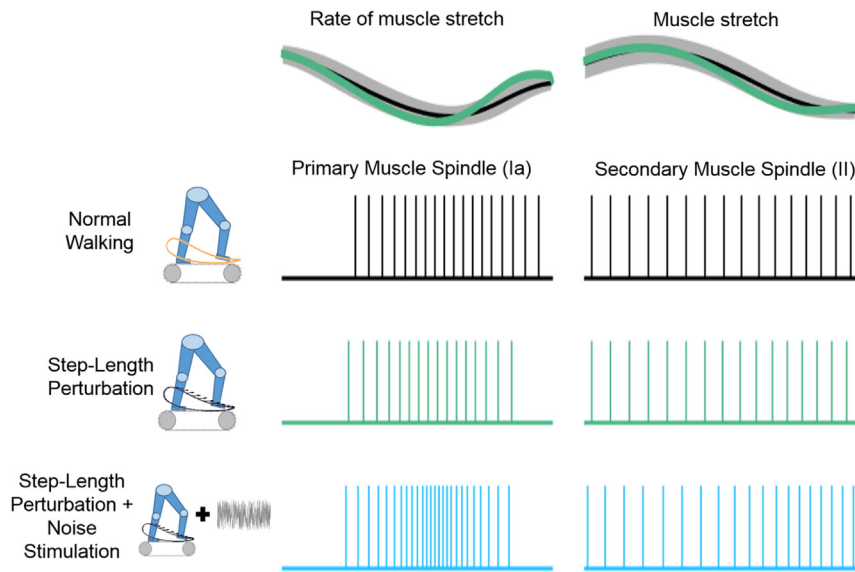
Figure 5. Theoretical model of the effect of subsensory electrical stimulation on the spindles of the hamstring muscles during the locomotor adaptation experiments

The response of primary muscle spindles (afferent Ia) is modeled as a firing depending on the rate of muscle stretch (modeled, for the hamstring muscle during swing, as the derivative of the knee angle, top plot, left), whereas the response of the secondary muscle spindles (afferent II) is modeled as a firing directly dependent on the amount of muscle stretch (modeled as the changes in knee angle, top plot, right). The perturbation (third row) leads to increased firing rate during late swing phase for both the Ia and II afferents. The effect of the subsensory stimulation is that of increasing the depolarization level of the spindles, affecting the firing/stretch relationship for both the Ia and II receptors. During subsensory electrical stimulation higher firing rates are associated with the same stretch and rate of stretchy induced by the perturbation, possibly altering the active response of the muscle through spinal and supra-spinal circuits.

leading the CNS to predict a higher biomechanical error, earlier during the swing phase. This effect could drive an anticipated higher activity in the hamstring muscles while compensating for the effects of the perturbation that would cause a faster adaptation similarly to what has been observed by Emken et al.[36]

At the same time, the disruption of the normal firing/stretch relationship in the II receptors could alter the perceived level of stretch thus modifying the perceived target adapted muscle length, inhibiting the activity of the hamstring earlier than in the non-stimulated condition. In the context of this interpretation, the overall faster rate of adaptation observed in the STIM condition would be both a primary effect of the stimulation and a secondary effect of the larger kinematic error observed at the end of adaptation. Our results support but do not confirm this theoretical framework, that needs to be verified through specifically designed experiments involving the recording of both spindle activity and surface EMG of the hamstring.

It is worth noticing that the STIM condition is also associated with a higher inter-subject step length variability that is not dependent on an increase in intra-subject variability. This behavior suggests a participant-specific response to the stimulation. For each participant, we selected the RMS value of the stimulating noise current equal to 90% of the sensory threshold. This value, selected based on the response of the skin nociceptors, may lead to different degrees of deeper muscle spindle depolarization across participants (also considering the differences, across participants in leg size, muscle tone and fat distribution), thus it may be "more optimal" for some individuals and less for others. This interpretation about the cause of the observed variability, could suggest the presence of a Stochastic Resonance effect associated with the noise stimulation, as suggested by several previous studies in literature,[1–4,8,10,18] where an optimal level of noise maximizes the operations of a threshold-base system, whereas smaller and higher levels of noise yield worse results. Future experiments could explore methods to optimize the stimulation level for an individual based on muscle spindle sensitization rather than skin sensation. It also needs to be pointed out that, in an electrical stimulation like the one that we administered in our experiments, the current is distributed over a large area, whereas spindles may be distributed also deep within the muscle tissue, in a subject-specific way. Thus, a different number of spindles may be affected by the stimulation across participants,

contributing to the variability in the response to the stimulation. Moreover, because of the lack of selectivity of the surface stimulation we cannot exclude that other neural pathways may be affected at the same time.

These results show that subsensory electrical stimulation directly modifies motor control during the performance of dynamic tasks, and that the observed kinematic effects are theoretically supported by a modification in activity of the stimulated muscle. Our findings could have interesting applications in gait rehabilitation. Our results, in fact, suggest that subsensory electrical stimulation can be used to modulate the activation of the targeted muscles in response to a stretch. Although it is not easy to predict if individuals with impaired proprioception would respond to the stimulation in the same way as we observed in healthy individuals, the ability to selectively modulate muscular response during training through peripheral proprioceptive enhancement could theoretically be useful in promoting targeted and individual-specific changes in muscular activity in response to the forces that the robot exerts on the leg.

Limitations of the study

The aim of the electrical stimulation we delivered to participants was to hyperpolarize muscle spindles. However, in the electrical stimulation protocol we administered in our experiments, the current is distributed over a large area, whereas spindles may be distributed also deep within the muscle tissue, in a subject-specific way. Thus, a different number of spindles may be affected by the stimulation across participants, contributing to the variability in the response to the stimulation. Moreover, because of the lack of selectivity of the surface stimulation we cannot exclude that other neural pathways may be affected at the same time.

STAR★METHODS

Detailed methods are provided in the online version of this paper and include the following:

- KEY RESOURCES TABLE
- RESOURCE AVAILABILITY
  - Lead contact
  - Materials availability
  - Data and code availability
- EXPERIMENTAL MODEL AND SUBJECT DETAILS
  - Participants and ethics statement
- METHOD DETAILS
  - Experimental Setup and sessions
  - Locomotor adaptation experiment
  - The perturbation
  - Electrical stimulation
- QUANTIFICATION AND STATISTICAL ANALYSIS
  - Data analysis

SUPPLEMENTAL INFORMATION

Supplemental information can be found online at https://doi.org/10.1016/j.isci.2023.107038.

AUTHOR CONTRIBUTIONS

Conceptualization: P.B. and J.N.; Methodology: G.S., A.K., I.C., J.N., and P.B.; Investigation: G.S., A.K., and I.C.; Visualization: G.S.; Supervision: P.B. and J.N.; Writing–original draft: G.S. and P.B.; Writing–review and editing: A.K., I.C., and J.N.

DECLARATION OF INTERESTS

JN is currently a technical advisor to Accelera, a US-based early state company looking to develop products using stochastic resonance stimulation to improve neurological deficits in patients. PB has received grant

REFERENCES

1. Priplata, A.A., Patritti, B.L., Niemi, J.B., Hughes, R., Gravelle, D.C., Lipsitz, L.A., Veves, A., Stein, J., Bonato, P., and Collins, J.J. (2006). Noise-enhanced balance control in patients with diabetes and patients with stroke. Ann. Neurol. 59, 4–12. https://doi.org/10.1002/ana.20670.

2. Gravelle, D.C., Laughton, C.A., Dhruv, N.T., Katdare, K.D., Niemi, J.B., Lipsitz, L.A., and Collins, J.J. (2002). Noise-enhanced balance control in older adults. Neuroreport 13, 1853–1856. https://doi.org/10.1097/00001756-200210280-00004.

3. Priplata, A., Niemi, J., Salen, M., Harry, J., Lipsitz, L.A., and Collins, J.J. (2002). Noise-Enhanced human balance control. Phys. Rev. Lett. 89, 238101–238106. https://doi.org/10.1103/PhysRevLett.89.238101.

4. Miranda, D.L., Hsu, W.H., Gravelle, D.C., Petersen, K., Ryzman, R., Niemi, J., and Lesniewski-Laas, N. (2016). Sensory enhancing insoles improve athletic performance during a hexagonal agility task. J. Biomech. 49, 1058–1063. https://doi.org/10.1016/j.jbiomech.2016.02.022.

5. Collins, J.J., Chow, C.C., and Imhoff, T.T. (1995). Aperiodic stochastic resonance in excitable systems. Phys. Rev. E 52, R3321–R3324. https://doi.org/10.1103/PhysRevE.52.R3321.

6. Gammaitoni, L. (1995). Stochastic resonance and the dithering effect in threshold physical systems. Phys. Rev. E 52, 4691–4698. https://doi.org/10.1103/PhysRevE.52.4691.

7. Calim, A., Palabas, T., and Uzuntarla, M. (2021). Stochastic and vibrational resonance in complex networks of neurons. Philos. Trans. A Math. Phys. Eng. Sci. 379, 20200236. https://doi.org/10.1098/rsta.2020.0236.

8. Cordo, P., Inglis, J.T., Verschueren, S., Collins, J.J., Merfeld, D.M., Rosenblum, S., Buckley, S., and Moss, F. (1996). Noise in human muscle spindles. Nature 383, 769–770. https://doi.org/10.1038/383769a0.

9. Collins, J.J., Priplata, A.A., Gravelle, D.C., Niemi, J., Harry, J., and Lipsitz, L.A. (2003). Noise-Enhanced human sensorimotor function. IEEE Eng. Med. Biol. Mag. 22, 76–83. https://doi.org/10.1109/MEMB.2003.1195700.

10. Severini, G., and Delahunt, E. (2018). Effect of noise stimulation below and above sensory threshold on postural sway during a mildly challenging balance task. Gait Posture 63, 27–32. https://doi.org/10.1016/j.gaitpost.2018.04.031.

11. Magalhães, F.H., and Kohn, A.F. (2014). Effectiveness of electrical noise in reducing postural sway: a comparison between imperceptible stimulation applied to the anterior and to the posterior leg muscles. Eur. J. Appl. Physiol. 114, 1129–1141. https://doi.org/10.1007/s00421-014-2846-5.

12. Magalhães, F.H., and Kohn, A.F. (2012). Imperceptible electrical noise attenuates isometric plantar flexion force fluctuations with correlated reductions in postural sway. Exp. Brain Res. 217, 175–186. https://doi.org/10.1007/s00221-011-2983-6.

13. Likens, A.D., Kent, J.A., Sloan, C.I., Wurdeman, S.R., and Stergiou, N. (2020). Stochastic resonance reduces sway and gait variability in individuals with unilateral transtibial amputation: a pilot study. Front. Physiol. 11, 573700. https://doi.org/10.3389/fphys.2020.573700.

14. Chen, W.M., Li, J.W., Geng, X., Wang, C., Chen, L., and Ma, X. (2020). The potential influence of stochastic resonance vibrations on neuromuscular strategies and center of pressure sway during single-leg stance. Clin. Biomech. 77, 105069. https://doi.org/10.1016/j.clinbiomech.2020.105069.

15. Elfering, A., Schade, V., Stoecklin, L., Baur, S., Burger, C., and Radlinger, L. (2014). Stochastic resonance whole-body vibration improves postural control in health care professionals: a worksite randomized controlled trial. Work. Health Saf. 62, 187–196. https://doi.org/10.3928/21650799-20140422-04.

16. Toledo, D.R., Barela, J.A., and Kohn, A.F. (2017). Improved proprioceptive function by application of subsensory electrical noise: effects of aging and task-demand. Neuroscience 358, 103–114. https://doi.org/10.1016/j.neuroscience.2017.06.045.

17. Lipsitz, L.A., Lough, M., Niemi, J., Travison, T., Howlett, H., and Manor, B. (2015). A shoe insole delivering subsensory vibratory noise improves balance and gait in healthy elderly people. Arch. Phys. Med. Rehabil. 96, 432–439. https://doi.org/10.1016/j.apmr.2014.10.004.

18. Castronovo, A.M., Giles Doran, C., Holden, M., and Severini, G. (2019). Analysis of the effectiveness of sub-sensory electrical noise stimulation during visuomotor adaptations in different visual feedback conditions. Front. Bioeng. Biotechnol. 7, 399. https://doi.org/10.3389/fbioe.2019.00399.

19. Miranda, D.L., Hsu, W.H., Petersen, K., Fitzgibbons, S., Niemi, J., Lesniewski-Laas, N., and Walsh, C.J. (2016). Sensory enhancing insoles modify gait during inclined treadmill walking with load. Med. Sci. Sports Exerc. 48, 860–868. https://doi.org/10.1249/MSS.0000000000000831.

20. Acuña, S.A., Zunker, J.D., and Thelen, D.G. (2019). The effects of sub-threshold vibratory noise on visuomotor entrainment during human walking and standing in a virtual reality environment. Hum. Mov. Sci. 66, 587–599. https://doi.org/10.1016/j.humov.2019.06.009.

21. Stephen, D.G., Wilcox, B.J., Niemi, J.B., Franz, J.R., Kerrigan, D., and D'Andrea, S.E. (2012). Baseline-dependent effect of noise-enhanced insoles on gait variability in healthy elderly walkers. Gait Posture 36, 537–540. https://doi.org/10.1016/j.gaitpost.2012.05.014.

22. Lam, T., and Pearson, K.G. (2002). The role of proprioceptive feedback in the regulation and adaptation of locomotor activity. In Advances in Experimental Medicine and Biology. https://doi.org/10.1007/978-1-4615-0713-0_40.

23. Dietz, V., Müller, R., and Colombo, G. (2002). Locomotor activity in spinal man: significance of afferent input from joint and load receptors. Brain *125*, 2626–2634. https://doi.org/10.1093/brain/awf273.

24. Frigon, A., and Rossignol, S. (2006). Experiments and models of sensorimotor interactions during locomotion. Biol. Cybern. *95*, 607–627. https://doi.org/10.1007/s00422-006-0129-x.

25. Nielsen, J.B., and Sinkjaer, T. (2002). Afferent feedback in the control of human gait. J. Electromyogr. Kinesiol. *12*, 213–217. https://doi.org/10.1016/S1050-6411(02)00023-8.

26. Rossi, C., Bastian, A.J., and Therrien, A.S. (2021). Mechanisms of proprioceptive realignment in human motor learning. Curr. Opin. Physiol. *20*, 186–197. https://doi.org/10.1016/j.cophys.2021.01.011.

27. Sombric, C., Gonzalez-Rubio, M., and Torres-Oviedo, G. (2019). Split-Belt walking induces changes in active, but not passive, perception of step length. Sci. Rep. *9*, 16442. https://doi.org/10.1038/s41598-019-52860-9.

28. Leech, K.A., Day, K.A., Roemmich, R.T., and Bastian, A.J. (2018). Movement and perception recalibrate differently across multiple days of locomotor learning. J. Neurophysiol. *120*, 2130–2137. https://doi.org/10.1152/jn.00355.2018.

29. Statton, M.A., Vazquez, A., Morton, S.M., Vasudevan, E.V.L., and Bastian, A.J. (2018). Making sense of cerebellar contributions to perceptual and motor adaptation. Cerebellum *17*. https://doi.org/10.1007/s12311-017-0879-0.

30. Cajigas, I., Koenig, A., Severini, G., Smith, M., and Bonato, P. (2017). Robot-induced perturbations of human walking reveal a selective generation of motor adaptation. Sci. Robot. *2*, eaam7749. https://doi.org/10.1126/scirobotics.aam7749.

31. Severini, G., Koenig, A., Adans-Dester, C., Cajigas, I., Cheung, V.C.K., and Bonato, P. (2020). Robot-driven locomotor perturbations reveal synergy-mediated, context-dependent feedforward and feedback mechanisms of adaptation. Sci. Rep. *10*, 5104. https://doi.org/10.1038/s41598-020-61231-8.

32. Jezernik, S., Colombo, G., Keller, T., Frueh, H., and Morari, M. (2003). Robotic orthosis Lokomat: a rehabilitation and Research tool. Neuromodulation *6*, 108–115. https://doi.org/10.1046/j.1525-1403.2003.03017.x.

33. Malone, L.A., Vasudevan, E.V.L., and Bastian, A.J. (2011). Motor adaptation training for faster relearning. J. Neurosci. *31*, 15136–15143. https://doi.org/10.1523/JNEUROSCI.1367-11.2011.

34. Lam, T., Anderschitz, M., and Dietz, V. (2006). Contribution of feedback and feedforward strategies to locomotor adaptations. J. Neurophysiol. *95*, 766–773. https://doi.org/10.1152/jn.00473.2005.

35. Emken, J.L., Benitez, R., Sideris, A., Bobrow, J.E., and Reinkensmeyer, D.J. (2007). Motor adaptation as a greedy optimization of error and effort. J. Neurophysiol. *97*, 3997–4006. https://doi.org/10.1152/jn.01095.2006.

36. Emken, J.L., and Reinkensmeyer, D.J. (2005). Robot-enhanced motor learning: accelerating internal model formation during locomotion by transient dynamic amplification. IEEE Trans. Neural Syst. Rehabil. Eng. *13*, 33–39. https://doi.org/10.1109/TNSRE.2004.843173.

37. Ruitenberg, M.F.L., De Dios, Y.E., Gadd, N.E., Wood, S.J., Reuter-Lorenz, P.A., Kofman, I., Bloomberg, J.J., Mulavara, A.P., and Seidler, R.D. (2018). Multi-day adaptation and savings in manual and locomotor tasks. J. Mot. Behav. *50*, 517–527. https://doi.org/10.1080/00222895.2017.1371110.

38. Enoka, R.M. (2015). Neuromechanics of Human Movement. https://doi.org/10.5040/9781492595632.

39. Duschau-Wicke, A., Von Zitzewitz, J., Caprez, A., Lünenburger, L., and Riener, R. (2010). Path control: a method for patient-cooperative robot-aided gait rehabilitation. IEEE Trans. Neural Syst. Rehabil. Eng. *18*, 38–48. https://doi.org/10.1109/TNSRE.2009.2033061.

40. Aoyagi, D., Ichinose, W.E., Harkema, S.J., Reinkensmeyer, D.J., and Bobrow, J.E. (2007). A robot and control algorithm that can synchronously assist in naturalistic motion during body-weight-supported gait training following neurologic injury. IEEE Trans. Neural Syst. Rehabil. Eng. *15*, 387–400. https://doi.org/10.1109/TNSRE.2007.903922.

41. Vallery, H., Duschau-Wicke, A., and Riener, R. (2010). Hiding robot inertia using resonance. In 2010 Annual International Conference of the IEEE Engineering in Medicine and Biology Society, EMBC'10. https://doi.org/10.1109/IEMBS.2010.5626416.

STAR★METHODS

KEY RESOURCES TABLE

REAGENT or RESOURCE	SOURCE	IDENTIFIER
Software and algorithms		
MATLAB 2021a	MathWorks	www.mathworks.com

RESOURCE AVAILABILITY

Lead contact

Further information and requests for resources should be directed to and will be fulfilled by the lead contact, Giacomo Severini (giacomo.severini@ucd.ie).

Materials availability

This study did not generate new unique reagents.

Data and code availability

- Data will be shared by the lead contact upon request.

- Code will be shared by the lead contact upon request.

- Any additional information required to reanalyze the data reported in this paper is available from the lead contact upon request.

EXPERIMENTAL MODEL AND SUBJECT DETAILS

Participants and ethics statement

30 healthy individuals (15 women, average age = 27.4 $\pm$ 3.8, average BMI = 22.9 $\pm$ 2) participated in this study. Among the participants, 6 had experienced the Locomotor adaptation experiment at least once before the beginning of the study, but each more than one month before the first experimental session. All procedures were performed at the Spaulding Rehabilitation Hospital in Boston. All experimental protocols were approved by the Spaulding Rehabilitation Hospital Internal Review Board.

METHOD DETAILS

Experimental Setup and sessions

The study consisted of three experimental sessions. All experimental sessions were performed using the Lokomat (Hocoma AG, Switzerland) exoskeleton. The Lokomat consists of a lower limb exoskeleton attached to a frame that allows for actuation of hips and knees while the participant walks on a treadmill. The Lokomat system allows for Body Weight Support, although this feature was not used during the experiments. The Path Control modality allows participants to naturally control the timing of their gait while using the machine.[39] This is achieved by estimating, at every instant, the current phase of the gait cycle by comparing the actual joint position and velocities with a pre-determined pattern using the algorithm developed by Aoyagi and colleagues.[40] For each participant, the experimental sessions were held on different days, with a maximum of 10 days between the first and the last session and at least one day of rest between consecutive Locomotor adaptation experiments.

The first experimental session was used to find the settings for correctly fitting the person inside the Lokomat. During the first session participants walked while attached to the Lokomat for approximately 10 minutes and were familiarized with walking while attached to the device. During the second and third sessions the participants underwent the Locomotor adaptation Experiments, once while experiencing continuous subsensory electrical stimulation during the whole experiment (STIM) and once with electrical stimulation only in the first 20 seconds of the experiment (NOSTIM). The order of the STIM and NOSTIM experiments was randomized across participants with 15 participants (STIM-First group) performing the STIM experiment in the second session (first Locomotor adaptation Experiment) and 15 participants (NOSTIM-First group) performing the STIM experiment in the third session (second Locomotor adaptation Experiment).

Locomotor adaptation experiment

After the initial setup, participants went through a *pre-baseline* part that consisted of two phases. In the first phase, participants were asked to walk for 90 seconds at 3 km/h with the machine back-driven (thus interaction forces between the Lokomat and the participant were minimized in order to give the impression of "free walking"). The data recorded during this period were used to calculate the Generalized Elasticities[41] that allow for the minimization of the device loading during operations. In the second phase participants were asked to walk for 120 seconds in back-driven mode (but with the newly updated elasticity) in order to record their baseline walking pattern. This baseline pattern was used as reference for the Aoyagi algorithm. After the *pre-baseline* part, which was repeated in each experimental session, participants performed the Locomotor adaptation experiment consisting of four consecutive blocks.

- **Catch trials:** 180 gait cycles, with the machine in back-driven mode. The perturbation was activated for 10 random single steps (catch trials) interspersed at least 8 steps between one another. These catch trials were used to estimate the "free" response to the perturbation, before adaptation can take place.

- **Baseline:** 80 gait cycles, with the machine in back-driven mode.

- **Force-Field:** 80 gait cycles, with the machine perturbing the participant's gait pattern through a velocity-dependent force field applied to the right leg during swing phase.

- **After-Effect:** 80 gait cycles with the machine in back-driven mode again.

Each Locomotor adaptation experiment lasted for about 10 minutes. During all the phases of the experiment (pre-baseline and adaptation experiment) the treadmill of the Lokomat was set to 3 km/h and participants were asked to follow the beat of a metronome pacing them at one full gait cycle every 1.4 seconds (85.7 bpm). All experimental procedures, including the setup of the Lokomat and the perturbation (see below), were identical to one of the experiments (the one labeled "X experiment") performed in our previously published study.[30]

The perturbation

The perturbation was designed as a velocity-dependent force field acting unilaterally on the right leg. The perturbation was active during the swing phase of the right foot and aimed at increasing the step-length of the participant experiencing it (see Figure 1). The perturbation force was generated by the robot according to the following equation:

$$F(t) = \begin{bmatrix} F_x(t) \\ F_y(t) \end{bmatrix} = \begin{bmatrix} A & 0 \\ B & 0 \end{bmatrix} \begin{bmatrix} v_x(t) \\ v_y(t) \end{bmatrix} \qquad \text{(Equation 1)}$$

where F_x and F_y represent the antero-posterior (*x*) and vertical (*y*) components of the perturbing force acting on the foot, and V_x and V_y represent the *x*- and *y*-components of the foot velocity as reconstructed using the following Jacobian:

$$J(\theta) = \begin{bmatrix} l_{Femur}\cos(\theta_h) + l_{tibia}\cos(\theta_h - \theta_k) & -l_{tibia}\cos(\theta_h - \theta_k) \\ l_{Femur}\sin(\theta_h) + l_{tibia}\sin(\theta_h - \theta_k) & -l_{tibia}\sin(\theta_h - \theta_k) \end{bmatrix} \qquad \text{(Equation 2)}$$

where l_{Femur} is the length of the femur, l_{Tibia} is the length of the tibia, and Θ is the vector of the joint angles Θ_h at the hip and Θ_k at the knee.

The damping coefficients were calculated as

$$A = 0.115 \cdot cos(\propto) \cdot Sm, B = 0.690 \cdot sin(\propto) \cdot Sm \qquad \text{(Equation 3)}$$

Where $\propto$ is the angle of the perturbation and *Sm* is the participant's mass in kg. For this experiment the angle was set at 8°. This angle was found, in our previous experiments,[30] as the angle at which the effect of the perturbation only act in the positive step length direction, without affecting the step height. The constant values in A and B were also empirically determined in the same experiment as values able to induce approximately a 30% increase in step length with respect to the baseline trajectory. The perturbation was applied only during the swing phase starting at the point of the gait cycle when the estimated foot velocity in the antero-posterior direction turned from negative to positive ($V_x(t) > 0|_{V_{x(t-1)} < 0}$) and ending at the point when the position of the foot in the antero-posterior direction turned from positive

to negative (x(t) < 0|$_{x(t-1)>0}$). The zero of the foot position in the antero-posterior direction was set at the center of the hip joint (Figure 1, Panel A).

Electrical stimulation

During both the STIM and NOSTIM experiments electrical noise stimulation was applied through surface electrodes placed above the hamstring muscles (Figure 1, Panel B). The electrodes were rectangular self-adhesive gel pads (Axelgaard Mfg. Co., Ltd., Fallbrook, CA, USA) placed approximately 5 cm above and below the upper cuff of the Lokomat. The electrical stimulation was Gaussian White Noise with zero mean and fixed root mean square (RMS) electrical current and was generated using a custom-developed isolated stimulator commanded via a custom software application. The frequency of the stimulation was between close to 0 Hz and 1 kHz. The RMS value of the electrical noise was set for each trial of each participant at 90% the RMS corresponding with the sensory threshold of the participant, where the sensory threshold is defined as the minimum RMS for which the participants were able to feel the stimulation on their skin. The sensory threshold was estimated for each participant before the beginning of each experiment. Specifically, after the participants were secured to the Lokomat system and before the beginning of the pre-baseline walking trials, the electrodes were placed on the skin and the procedure for defining the sensory threshold was initiated. A first check on the placement of the electrode was performed by applying a noise current with an RMS of 500 μA (that represented the upper limit of the possible RMS values), to check if participant could feel the stimulation and to show them the tickling sensation associated with a noise stimulation above the sensory threshold level. Next, we set the RMS of the noise stimulation at 20 μA and increased the value by 10 μA every 10 seconds until the participant reported a tickling sensation on the skin. The RMS of the electrical noise stimulation for the trial was then set at 90% this value. During the NOSTIM condition the subsensory electrical noise stimulation was applied only at the very beginning of the experiment, during the first 20 seconds of the Catch Trials phase. In the STIM condition the stimulation was applied during the whole experiment. Participants were told, before each session, that electrical noise stimulation may be applied to them during the Lokomat experiment. Since the stimulation was always below sensory threshold, participants were effectively blinded on the experimental condition during each experimental session.

QUANTIFICATION AND STATISTICAL ANALYSIS

Data analysis

The Lokomat system is equipped with 4 position and 4 torque sensors measuring respectively the joint angles and the interaction torques between the machine and the user at the hips and knees for both legs. The torque exerted by the participant during the experiments was calculated by subtracting the perturbation torques (calculated from Equation 4) from the interaction torques measured by the sensors. Since the effect of the perturbation administered during the Locomotor adaptation experiment was that of increasing the step length of the participants, adaptation and de-adaptation were evaluated for each participant in term of changes in the normalized value of step length. Step length was calculated from Equation 3 as the maximum value observed for the *x* variable during each gait pattern. The zero step-length value was set at the center of the hip joint (Figure 1, panel A). For each experiment of each participant, the step length associated with each step was normalized by dividing it by the average step length during the Baseline part of the experiment. Locomotor adaptation is commonly characterized by an exponential change in the kinematic/kinetic metric of interest.[30,31] We observed a similar behavior also in the Locomotor adaptation Experiments performed in this study (Figure 1, Panel C). Exponential fitting was applied on the force-field and after-effect sessions of the experiments according to the following formula:

$$f(n) = \alpha e^{-\beta n} + \gamma \qquad \text{(Equation 4)}$$

For the Force-field phase the parameter α, that represents the initial response to the perturbation, was estimated as the average of the deviations observed during the 9 single-step perturbations the participants experienced during the catch trial session of the experiment, which represent a "free" response to the perturbation before adaptation kicks in. The parameters β and γ, that represent respectively the time constant of the adaptation and the residual deviation at the end of the force-field phase, were estimated using a least-squares algorithm. For the after-effect phase, all the three parameters α, β and γ, were estimated, with 95% confidence intervals, using a least-squares algorithm. Exponential fitting was applied to the normalized step length patterns averaged across all participants for both conditions (STIM and NOSTIM) and across groups of participants stratified depending on the whether they performed the

STIM or NOSTIM experiments as the first Motor Adaption Experiment (STIM-First and NOSTIM-First groups). For all the analyses, the quality of the fitting was evaluated using the root mean squared error. The analysis of adaptation speed, estimated from the fittings as three times the value of the parameter β was used to verify our hypothesis that the stimulation leads to faster adaptation.

A series of additional analyses were run to characterize stimulation-dependent differences in the patterns of adaptation. Statistical analyses were performed to assess for significant ($p < 0.05$, after correction for multiple comparisons) differences between the step length values in different sessions of the experiments for both STIM and NOSTIM conditions. This analysis was based on Wilcoxon's signed rank test with Bonferroni-Holm correction that has been used to compare the values of step length between the STIM and NOSTIM conditions in three specific points of the experiments. Specifically, we analyzed: a) the first step of Force-Field, to investigate the presence of differences in initial response to the perturbation between the two conditions; b) the average of the last five steps of Force-field, to assess for differences between the two conditions when the adaptation is complete; c) the first step of After-Effect, to assess for differences in the starting point of the de-adaptation period.

We evaluated inter-subject and intra-subject variability in step length at the end of the force-field, when adaptation is supposed to be complete. The former measures the variability observed in each condition across the different participants, the latter measures the step-to-step variability of each participant for each condition. Inter-subject variability was calculated as the standard deviation (across participants) of the average step length calculated in the last thirty steps of the force-field phase. Intra-subject variability was instead calculated as the average standard deviation observed for each participant in the last thirty step of the force-field phase. Power was estimated, for both the hip and knee, from Equation 5:

$$W = \tau_{joint} \cdot \Delta\theta_{joint} \qquad \text{(Equation 5)}$$

Where τ_{joint} is the interaction torque measured at the joint and $\Delta\theta_{joint}$ is the joint angular velocity. We analyzed the differences among STIM and NOSTIM conditions in the power W_{add} needed to counteract the perturbation. This value was estimated, for each joint, as:

$$W_{add} = W_{late\ FF} - W_{late\ BL} - W_{perturbation} \qquad \text{(Equation 6)}$$

Were $W_{late\ FF}$ is the power estimated in the last ten steps of the Force-field phase, $W_{late\ BL}$ is the power estimated in the last ten steps of the Baseline phase and $W_{perturbation}$ is the power that is attributed to the perturbation. This value was estimated as:

$$W_{perturbation} = \tau_{Pert} \cdot \Delta(\theta_{CT} - \theta_{BL}) \qquad \text{(Equation 7)}$$

Where τ_{Pert} is the perturbing torque calculated in Equation 4 and θ_{CT} and θ_{BL} represent, respectively, the joint angles during the catch trials (where adaptation to the perturbation is not yet present) and the average angle measured during the Baseline condition.